Propene epoxidation with H_2 and O_2 on Au/TS-1 catalyst: Cost-effective synthesis of small-sized mesoporous TS-1 and its unique performance

Zhaoning Song[a], Xiang Feng[a,b,*], Nan Sheng[a], Dong Lin[a], Yichuan Li[a], Yibin Liu[a], Xiaobo Chen[a], Xinggui Zhou[b], De Chen[c] and Chaohe Yang[a]

[a] *State Key Laboratory of Heavy Oil Processing, School of Chemical Engineering, China University of Petroleum, Qingdao 266580, China.*

[b] *State Key Laboratory of Chemical Engineering, East China University of Science and Technology, Shanghai 200237, China.*

[c] *Department of Chemical Engineering, Norwegian University of Science and Technology, Trondheim 7491, Norway.*

Abstract: Designing cost-effective titanium silicalite-1 (TS-1) with enhanced mass transfer ability is of prime scientific and industrial importance. In this work, a novel small-sized mesoporous TS-1 (STS-1) material is first synthesized in cheap TPABr system using steam-assisted crystallization method. Compared with cheap microporous TS-1 prepared by classical hydrothermal method (HTS-1) with particle size of 950nm, STS-1 shows mesoporous character of 13 nm and reduced average particle size of 590 nm. Moreover, effect of TPABr concentration is systematically investigated, and both of insufficient and overmuch TPABr concentrations are unfavorable because of low crystallinity and exorbitant price, respectively. Importantly, the catalytic performance of cost-effective Au/STS-1 for direct propene epoxidation with H_2 and O_2 is much better than that of Au/HTS-1, and comparable to the performance of the expensive Au/TS-1. By multi-characterizations and activation energy analysis, the underlying mechanism for the enhanced performance is further discussed. This work sheds new light on the design and synthesis of highly effective and cost-efficient TS-1 catalysts.

Keywords: Cost-effective; TS-1; Particle size; TPABr; Propene epoxidation.

1 Introduction

Since titanium silicalite-1 (TS-1) was first synthesized by Taramasso et al. in 1983 [1], it has triggered extensive research attention arising from the unique physico-chemical properties, such as microporous channels with the diameter of ca. 0.55 nm and only the presence of isolated tetrahedral titanium species in the MFI framework [2]. As a consequence, TS-1 as a support or catalyst has exhibited attractive catalytic activity and selectivity in a series of sustainable selective oxidation reactions, for instance, epoxidation of alkenes [3,4], ammoximation of ketone [5,6], aromatic hydroxylation [7] and oxidation of alcohols and alkanes [8,9]. Take propene epoxidation for example, compared with traditional technological processes such as chlorohydrin and co-oxidation methods, direct gas phase propene epoxidation with H_2 and O_2 on Au/TS-1 catalyst has green, simple and sustainable merits to synthesize propylene oxide (PO). Therefore, developing efficient TS-1 material for the green selective oxidation reactions harbours tremendous potential for future industry and still needs to be extensively explored.

By traditional hydrothermal synthesis method, TS-1 with small crystalline size (200-500 nm) can be successfully synthesized using tetrapropylammonium hydroxide (TPAOH) as the organic template. However, the expensive TPAOH template significantly increases the synthetic cost, hindering the extensive application of TS-1 in industrial process. In recent years, many researchers have focused on the low-cost synthesis of TS-1 using inexpensive tetrapropylammonium bromide (TPABr) as organic template [10-12]. However, the as-synthesized TS-1 usually shows a large particle size over 1 μm. It is widely accepted that large zeolite crystals could impose significant diffusion limitations, impeding the transport of reactants and products inside the porous channels and leading to reduced activity,

selectivity and catalytic lifetime [13]. Therefore, reducing the crystal size of low-cost TS-1 is of prime industrial and scientific importance.

Compared with classical hydrothermal method, the steam-assisted crystallization (SAC) method is considered as a non-conventional synthesis approach to synthesize zeolitic small crystals. This method includes the preliminary preparation of an initial zeolite yielding gel, which is subsequently dried and then crystallized in vapor phase [14]. Several aluminophosphate and aluminosilicate zeolites with excellent catalytic performance have been successfully synthesized by SAC method [15-18]. On the one hand, this method can promote the nucleation process during the zeolite synthesis, which is advantageous to prepare small crystals. On the other hand, the SAC method usually shows higher yield than typical hydrothermal method. It also generates less waste and requires smaller volume of reactor [19]. However, little attention has been paid to synthesizing cost-effective and small-sized TS-1 by SAC method. Therefore, it is imperative to prepare active and cost-effective TS-1 catalysts based on the SAC method, which is also highly desired to the rational design of effective Au/Ti-containing catalysts for direct propene epoxidation.

In this work, we devise a cost-effective route to synthesize the novel small-sized mesoporous TS-1 (STS-1) by SAC method. TPABr as the cheap template is used to replace expensive TPAOH, and conventional TS-1 crystals are used as the seeds. It is found that the average particle size of STS-1 is smaller than that of HTS-1 which is also synthesized in the TPABr system by classical hydrothermal method. Meanwhile, the mesopores of ca. 13 nm are observed, which could facilitate the mass-transfer ability of catalyst. In addition, the effect of TPABr concentration is also studied to balance the relationship among crystallinity, particle size, Ti species and price. Furthermore, the performance of Au/STS-

1 catalyst is not only much better than Au/HTS-1, but also comparable to the expensive Au/TS-1 for direct propene epoxidation with H_2 and O_2. By activation energy analysis, multi-characterizations (e.g., HRTEM, UV-vis, FT-IR, SEM, N_2 physisorption and XRD) and experimental data, the underlying mechanism for the enhanced performance is also discussed. This work will be of referential importance to the rational design of efficient and cost-effective industrial TS-1 catalysts for epoxidation reactions.

2 Experimental

2.1 Catalyst Preparation

The synthetic procedures of HTS-1 support by hydrothermal method [20] was as follows: 0.76 g TPABr was dissolved in deionized water under stirring for 30 min. To the above solution, 2.8 g n-butylamine was added to adjust the alkalinity of the mixture to pH=12. This was followed by the addition of 9.5 g colloidal silica. Meanwhile, 0.26 g TBOT and 15ml isopropanol solution were stirred at room temperature for 1.5 h. The mixture was added to the hydrolyzed solution of colloidal silica dropwise under vigorous stirring. Subsequently, 0.2 g TS-1 seeds were added to the aforementioned solution and the solution was stirred for another 2 h at 353 K. The resulting mixture was placed into a Teflon-lined stainless-steel autoclave and crystallized at 443 K for 72 h. Finally, the product was washed and centrifuged with distilled water, dried at 353 K overnight and calcined at 823 K for 6 h. The molar composition of the gel was as follows: SiO_2: TiO_2: TPABr: n-butylamine: H_2O= 1.0: 0.016: 0.03-0.18: 0.8: 30.

In contrast, the synthesis of STS-1 by steam-assisted crystallization (SAC) method was similar to hydrothermal method except for the crystallization procedure. The same amount

of TPABr, NBA, colloidal silica, TBOT and TS-1 seeds were mixed firstly. After that, the obtained solution was stirred for 5 h at 353 K in a water bath, resulting in an amorphous dry gel. This dry gel was placed into a Teflon cup inside a Teflon-lined stainless-steel autoclave. Subsequently, an appropriate amount of deionized water was introduced to the bottom of steel autoclave. The dry gel was crystallized at 443 K for 72 h. At this temperature, the water steam was in close contact with the dry gel. Afterwards, the product was washed and centrifuged with distilled water, dried at 353 K overnight and calcined at 823 K for 6 h.

Au/STS-1 and Au/HTS-1 catalysts were prepared by the deposition-precipitation method [21]. 0.1 g hydrogen tetrachloroaurate (III) trihydrate ($HAuCl_4 3H_2O$, 99.99%) was mixed with 50 mL deionized water. 0.5 g TS-1 support was slowly added to the above solution. The mixture was stirred for 1 h at room temperature, and the slurry was then adjusted to the pH of 7.3-7.6 by 1 M and 0.1 M aqueous solution of NaOH and stirred at room temperature for 9 hours. The resulting catalyst was then separated by centrifugation (5000 rpm for 10 min), washed three times with 100ml deionized water and dried at 298K overnight under vacuum.

2.2 Characterization

The X-ray diffraction patterns (XRD) of TS-1 catalysts were collected on a X'pert PRO MPD diffractometer instrument using Cu-Kα radiation. The N_2 adsorption-desorption isotherms were measured on a Micromeritics ASAP 2020 instrument. The Fourier transform infrared spectroscopy (FT-IR) spectra of the catalysts were obtained on a Nicolet NEXUS 670 spectrometer with KBr as background. The ultraviolet-visible spectroscopy (UV-vis) spectra from 210 to 800 nm was determined on a PerkinElmer Lambda 35

spectrophotometer, and pure $BaSO_4$ was used as reference. Au loadings were determined by the inductive coupled plasma optical emission spectrometry (ICP-OES) on an Agilent 730 ICP-OES spectrometer. The high resolution transmission electron microscopy (HRTEM) images were taken on a JEOL JSM-2100F microscope, and the scanning electron microscopy (SEM) images were obtained on a Hitachi S-4800 field-emission scanning electron microscope.

2.3 Gas-phase propene epoxidation with H_2 and O_2

The gas-phase propene epoxidation with H_2 and O_2 was taken in a quartz tubular reactor (i.d. 8 mm) employing a feed containing C_3H_6, H_2, O_2 and N_2 with the flow rate of 3.5/3.5/3.5/24.5 mL·min-1. The Au/STS-1 and Au/HTS-1 catalysts (0.15 g) were tested under atmospheric pressure. The reactants and products were analyzed using two on-line GC (Fuli 9790). Hydrocarbons, H_2, O_2, N_2, COx and H_2O were analyzed by GC equipped with TCD. Oxygenates such as propylene oxide, ethanal, propanal, acetone and acrolein were analyzed by the other GC equipped with FID. Blank tests indicated that no PO was generated in the blank reactor.

A reaction temperature of 473 K was chosen for catalytic performance testing. Each Au/TS-1 catalyst was heated in the reaction mixture from room temperature to 473 K and lasted for more than 6 h at 473 K. The obtained PO formation rate and PO selectivity in this work were the average values between the 2nd to 3th h at 473 K."

Propylene conversion = mol of (C_3-oxygenates + 2/3ethanal + CO_2/3)/mol of propene in the feed.

PO selectivity = mol of PO/mol of (C_3-oxygenates + 2/3ethanal + CO_2/3).

3 Results and discussion

3.1 STS-1 synthesized by steam-assisted crystallization method

Novel small-sized mesoporous TS-1 sample (STS-1) is first synthesized using cheap TPABr as template by steam-assisted crystallization method. Fig. 1a shows the powder X-ray diffraction (XRD) patterns of STS-1 and HTS-1 samples with the TPABr/SiO_2 molar ratio of 0.18. It is clear that STS-1 and HTS-1 all show the characteristic diffraction peaks at 7.8°, 8.8°, 23.1°, 23.9°and 24.3°, indicating that both of the two samples have the typical MFI topological structure. Each of the sharp single diffraction peaks at $2\theta = 24.3°$ for the two samples indicates their orthorhombic symmetry rather than the monoclinic symmetry. In addition, both of the two samples show high crystallinity and the absence of additional peaks of amorphous structures. Moreover, it is also noted that compared with HTS-1, the STS-1 sample shows the broadening of XRD diffraction peaks. This indicates the reduction of TS-1 crystal size for STS-1 sample [22]. The N_2 adsorption-desorption isotherms and pore-size distributions of STS-1 and HTS-1 samples are shown in Fig. 1b. HTS-1 exhibits a typical type I isotherm according to IUPAC's classification, demonstrating the microporous characteristic. The neglectable uptake in the isotherm of HTS-1 at $P/P_0 > 0.1$ reveals the absence of mesoporosity. For STS-1 sample, the rapid elevation of the curve at $P/P_0 < 0.02$ indicates the existence of micropores. Moreover, the adsorption-desorption curves exhibit typical IUPAC type IV isotherms with a H4 hysteresis loop, which is characteristic of porous materials with narrow slit like wedge-shaped pores. The capillary condensation occurs at P/P_0 range of ca. 0.45 to 0.95 is observed, which is due to multilayer adsorption of nitrogen molecules inside mesopores. The corresponding pore-size

distribution indicates that the STS-1 sample not only has micropores with diameters of ca. 0.55 nm which is correspond to the pore size of typical TS-1, but also contains mesopores with diameters of ca. 13 nm. These consequences constitute the hierarchically porous structure in STS-1 crystal particle.

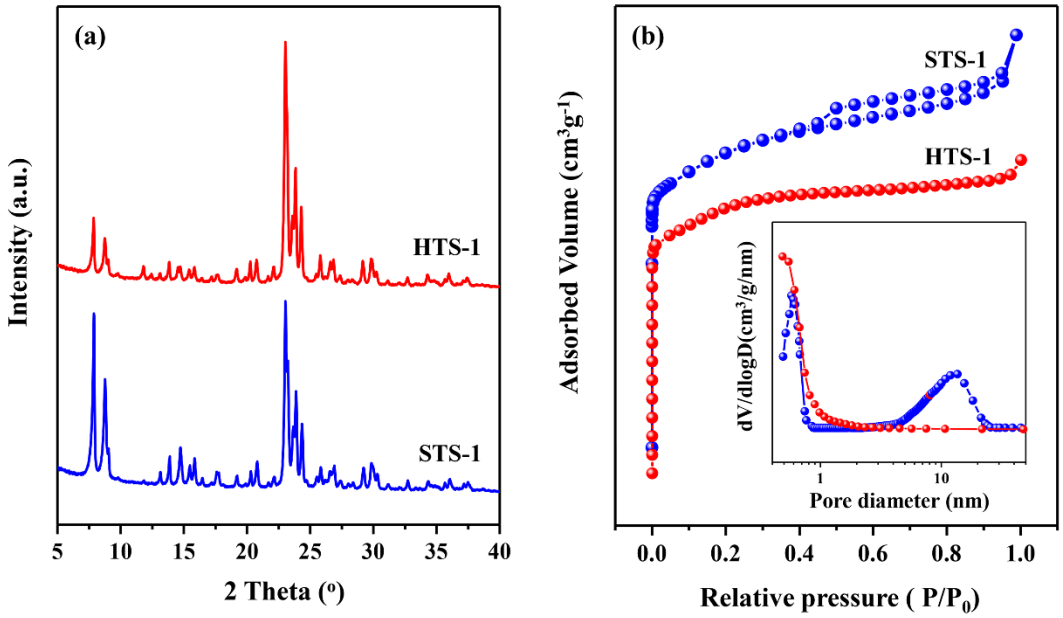

Fig. 1. (a) XRD spectra and (b) N_2 adsorption-desorption isotherms of STS-1 and HTS-1 samples. The inset in Fig.1b shows the pore size distributions.

For catalytic oxidation reactions such as propene epoxidation, ammoximation of ketone and aromatic hydroxylation, the existence of Ti species is indispensable [23-25]. The environment of Ti inside or outside the framework of TS-1 can be investigated by FT-IR and UV-vis characterizations. Fig. 2a shows the FT-IR spectra of STS-1 and HTS-1 samples. Results show that each sample exhibits six typical characteristic bands in the finger print region, i.e., 450, 550, 800, 960, 1100 and 1230 cm^{-1}. This is in accordance with the reported FT-IR spectra of typical TS-1 [26]. The adsorption bands at 450, 800 and 1100 cm^{-1} are attributed to the bend stretch, symmetrical and antisymmetrical stretching

vibration of [SiO_4] units, respectively. The bands at 550 and 1230 cm^{-1} are due to the vibration of double five-membered ring and asymmetrical stretching vibration of MFI framework structure [27]. It is noted that the adsorption band at 960 cm^{-1} indicates the presence of the Si-O-Ti structure inside the framework [28]. The result suggesting that titanium can be effectively introduced into the framework of both STS-1 and HTS-1.

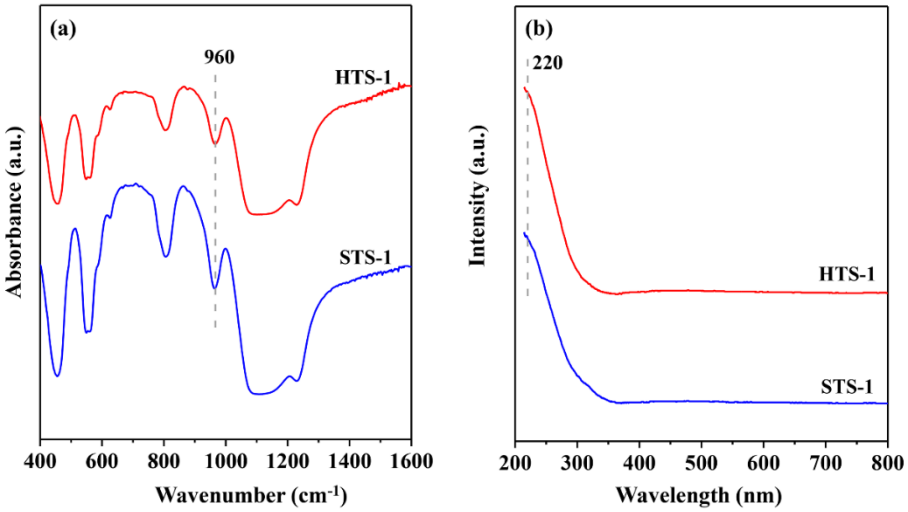

Fig. 2. (a) FT-IR and (b) UV-vis spectra of STS-1 and HTS-1 samples.

FT-IR could only be used to indicate the presence of Ti species inside the framework of TS-1. The detailed composition of Ti species should be further determined by UV-vis characterization. From Fig. 2b, it can be seen that there are dominating adsorption peaks at ca. 220 nm for the two samples, which are ascribed to the charge transfer from O^{2-} to Ti^{4+} [29,30]. This is the characteristic of isolated tetrahedrally coordinated Ti ion in the framework of TS-1. These isolated tetrahedrally coordinated Ti species inside TS-1 could usually play the role of oxidation and is essential for catalytic reactions [31]. No adsorption peaks at 250-280 and 330 nm are observed for both of the samples, indicating the absence of octahedrally coordinated Ti complexes and anatase TiO_2 species, respectively [32,33]. The FT-IR and UV-vis results show that the existence of Ti species in the framework of

STS-1 and HTS-1 samples are quite similar. This result excludes the influence factor of the titanium species between the two samples on the catalytic performance.

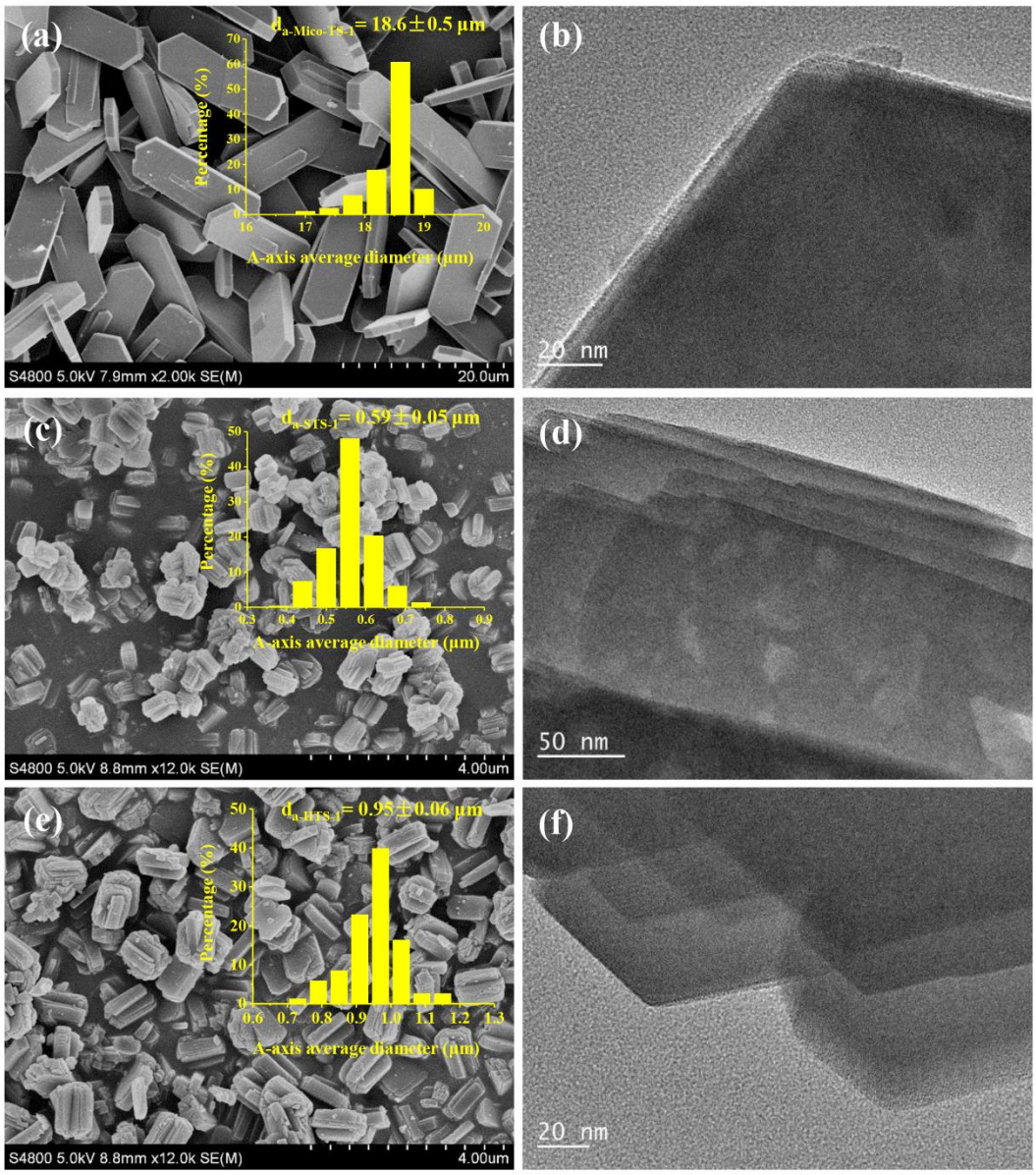

Fig. 3. Representative SEM and TEM images of (a-b) micron-sized TS-1, (c-d) STS-1 and (e-f) HTS-1. The insets show the crystal particle size distributions of a-axis.

Fig. 3 shows the typical SEM and TEM images of micron-sized TS-1, STS-1 and HTS-1 samples. When TS-1 is synthesized using TPABr as template by hydrothermal method

without adding seeds, the average crystal size is about 18.6*5.5*1.0 μm as shown in Fig. 3a. However, obvious reduction of average crystal size from 18.6*5.5*1.0 μm to 950*720*300 nm is observed when TS-1 is synthesized by hydrothermal method with seeds. The as-synthesized HTS-1 material is twin crystal morphology. This could be because the added TS-1 seeds serve as the TS-1 nuclei, which contribute to crystal growth by attachment [34]. In contrast, the STS-1 material synthesized by steam-assisted crystallization method has smaller average particle size of 590*500*200 nm although twin crystal morphology is also observed. A large number of crystal nucleus are formed at the early stage of the synthesis process and the slow growth of crystals after nucleation should be the main reason for the smaller particle size of STS-1 crystals prepared by the steam-assisted crystallization method [35,36]. Moreover, mesopores are present on the STS-1 sample (Fig. 3d). The average pore size is ca. 13 nm, which agrees well with the pore size estimated from the BJH pore size distribution of ca. 13 nm. According to the literature, the formation of the pore structure of STS-1 sample is probably attributed to the desilication by alkaline steam during the steam-assisted crystallization process [37].

3.2 Effect of TPABr/SiO_2 molar ratio on the physicochemical properties of STS-1

The TPABr/SiO_2 molar ratio, as an essential parameter during synthesis, could greatly affect the physico-chemical properties of TS-1 [38]. Fig. 4 shows the XRD patterns of STS-1 samples with different TPABr/SiO_2 molar ratios (i.e., 0.03, 0.06, 0.12 and 0.18). It can be seen that the all STS-1 samples exhibit typical MFI structure, as confirmed by characteristic diffraction peaks at 7.9°, 8.8°, 23.1°, 23.9° and also the single diffraction peaks at $2\theta = 24.3°$. However, very poor crystallization is observed at TPABr/SiO_2 ratio of

0.03 due to insufficient amount of TPA^+. When the $TPABr/SiO_2$ molar ratio is from 0.06 to 0.18, all samples show similar high crystallinity.

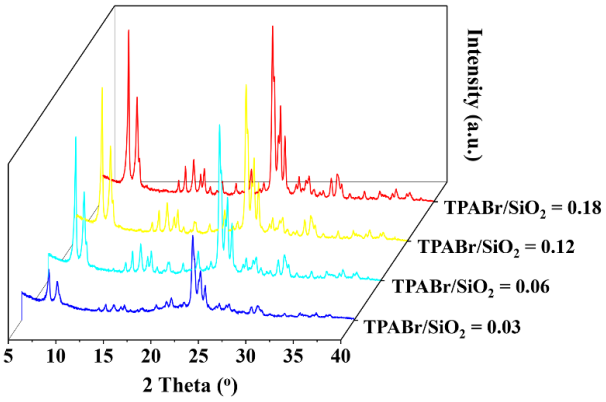

Fig. 4. XRD spectra of STS-1 with different $TPABr/SiO_2$ molar ratios.

Fig. 5 shows the FT-IR and UV-vis spectra of STS-1 samples with different $TPABr/SiO_2$ molar ratios. The peak at 960 cm^{-1} is ascribed to Si-O-Ti structure, which gradually decreases with the reduction of $TPABr/SiO_2$ molar ratios from 0.18 to 0.03. This indicates that Ti species could not easily enter into the framework of STS-1 when the concentration of TPABr template is reduced. This is also confirmed by the UV-vis spectra in Fig. 5b. From the UV-vis spectra, octahedrally coordinated Ti complexes and non-framework Ti species show up at $TPABr/SiO_2$ molar ratio of 0.03, indicating that the TPA^+ template is not sufficient during synthesis. At higher $TPABr/SiO_2$ ratios, the peaks at 250-280 nm and also 330 nm gradually disappear due to the positive effect of TPA^+ template. Meanwhile the adsorption peak at ca. 220 nm exists for all of the samples, confirming the presence of isolated Ti (IV) species in the MFI framework. The above results show that the insufficient TPABr concentration leads to the existence of non-framework Ti and anatase TiO_2 species in the framework, and the range of $TPABr/SiO_2$ molar ratio which is from 0.06 to 0.18 is appropriate for reaction.

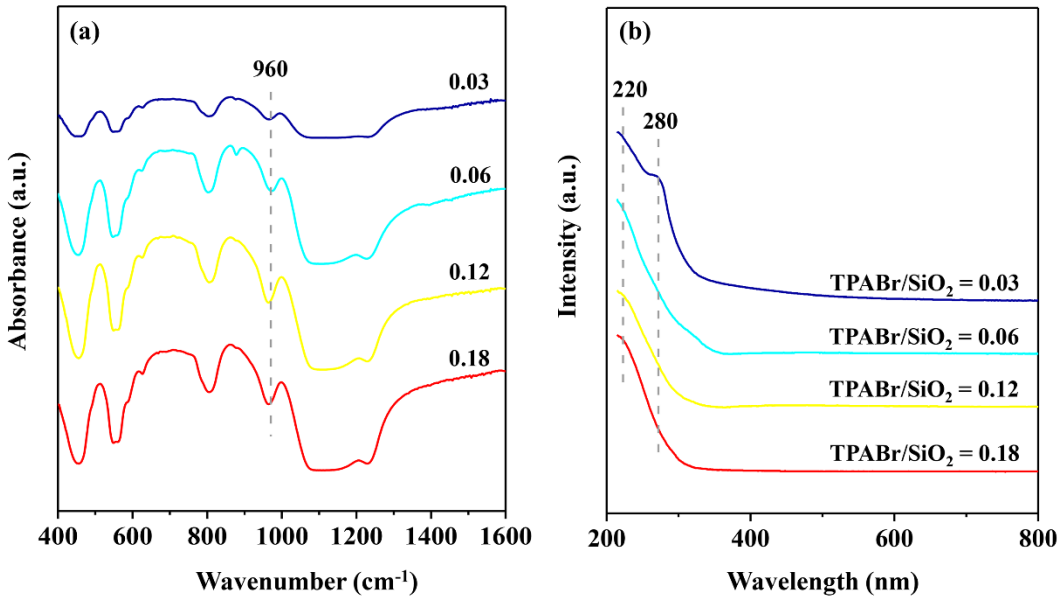

Fig. 5. (a) FT-IR and (b) UV-vis spectra of STS-1 with different TPABr/SiO_2 molar ratios.

Fig. 6 shows the typical SEM images of STS-1 samples with different TPABr/SiO_2 molar ratios. In accordance with the XRD results in Fig. 4, STS-1 with TPABr/SiO_2 molar ratio of 0.03 has low crystallinity and the absence of regular morphology. Only large aggregates of TS-1 can be observed in Fig. 6a. However, other samples with larger ratio exhibit good crystallinity and regular shape. The a-axis average particle size of STS-1 gradually increases from 590 to 670 nm with the decreases of TPABr/SiO_2 ratio from 0.18 to 0.06. This could be possible because that the higher TPABr concentration leads to the higher cationic surfactant concentration. Consequently, it becomes easier for tetrapropylammonium (TPA) cations to polymerize with the silicate anions, so as to form a large number of crystal nucleus in the early stages of synthesis and then reduce the crystal size [39,40].

According to the above results, the following conclusion can be obtained: the TPABr/SiO_2 molar ratio of 0.06 is not only useful to further reduce the synthetic cost of

TS-1, but also feasible to synthesize the small-sized mesoporous TS-1 with enough tetrahedrally coordinated Ti species. Therefore, the TPABr/SiO_2 molar ratio of 0.06 is considered to be the most appropriate template concentration

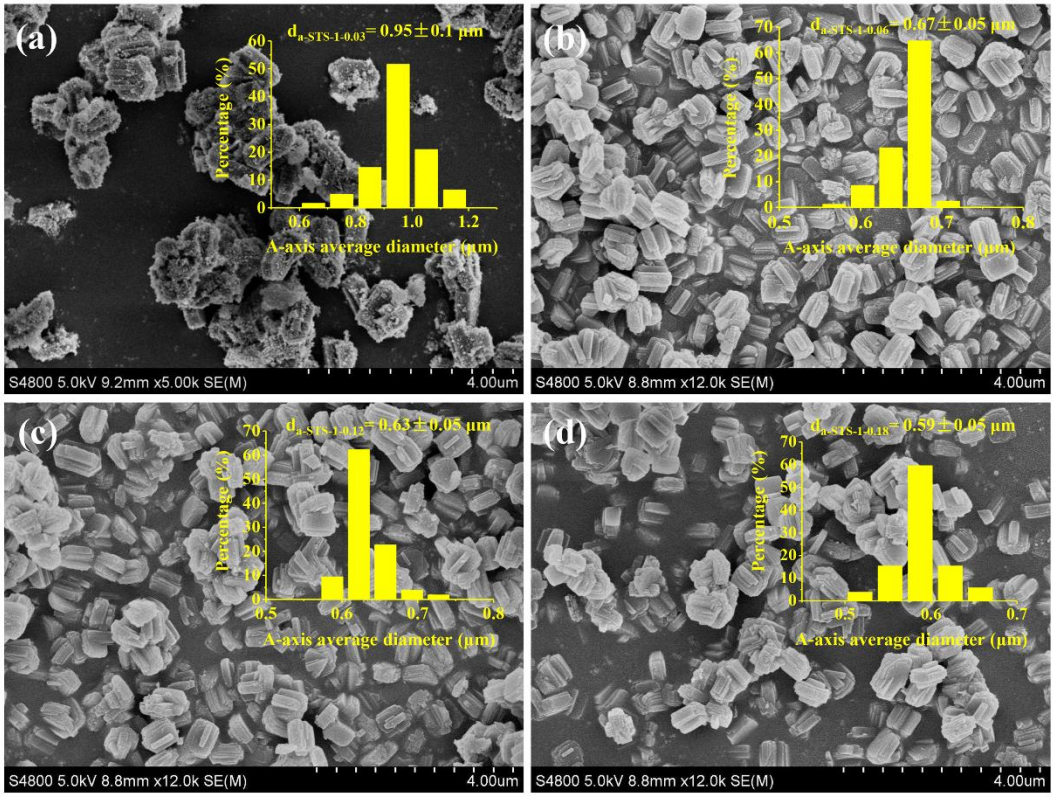

Fig. 6. Representative SEM images of STS-1 with TPABr/SiO_2 ratio of (a) 0.03, (b) 0.06, (c) 0.12 and (d) 0.18. The insets show the crystal particle size distributions of a-axis.

3.3 Catalytic performance of Au/STS-1 and Au/HTS-1 catalysts

Direct propene epoxidation with H_2 and O_2 to synthesize propylene oxide, as an essential industrial reaction to replace traditional chlorohydrin and peroxidation methods, has attracted much attention since 1998 [41]. For the reaction, titanium silicalite-1 supported Au catalyst shows superior catalytic performance than other catalysts [42-45]. Herein, STS-1 and HTS-1 with same TPABr/SiO_2 molar ratio of 0.06 are used as supports for Au

deposition. To make a fair comparison, the Au loadings of the two catalysts are similar (ca. 0.10 wt%).

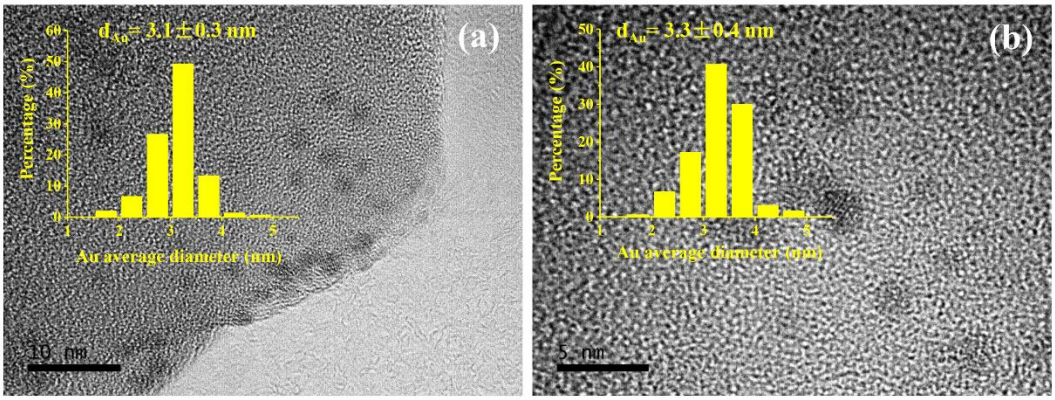

Fig. 7. HRTEM images of (a) Au/STS-1 and (b) Au/HTS-1 catalysts. The insets show the Au size distributions of the catalysts, and the scale bars represent 10nm and 5nm, respectively.

Fig. 7 shows the HRTEM images of the Au/STS-1 and Au/HTS-1 catalysts. More than 150 nanoparticles were measured to determine Au average particle size so as to increase accuracy. It is found that the Au/STS-1 and Au/HTS-1 catalysts show similar Au particle size of ca. 3.2 nm. This could exclude the effect of Au particle size [46,47] and give an intrinsic effect of support.

The catalytic performance of Au/STS-1, Au/HTS-1, Au/TS-1 and other Au/Ti-containing catalysts in literature for gas-phase propene epoxidation with H_2 and O_2 are compared in Table 1. It is clear that HTS-1 support with larger TS-1 particle size supported Au catalyst shows low PO formation rate and PO selectivity. However, Au/STS-1 catalyst exhibits good PO formation rate of 140.8 $g_{PO}h^{-1}kg_{Cat}^{-1}$ and slightly improved PO selectivity of 91.2%, which is quite similar with the reported conventional expensive Au/TS-1 catalyst at same Si/Ti molar ratio of 40 [48].

Table 1. The catalytic properties of Au/Ti-containing catalysts for gas-phase propene epoxidation.

Samples	Au loading (wt%)	PO selectivity (%)	PO formation rate ($g_{PO}h^{-1}kg_{Cat}^{-1}$)	Reaction temperature (K)	Reference
Au/STS-1[a]	0.10	91.2	141	473	This work
Au/HTS-1[a]	0.10	79.4	88	473	This work
Au/TS-1	0.10	90.0	150	473	[48]
Au/TS-1-Cs	0.16	88.8	320	473	[43]
Au/TS-1-SG	0.10	85.0	119	473	[49]
Au/TS-1-B	0.10	83	125	473	[21]
Au/NTS-1	0.08	84.4	104	423	[50]

[a] The supports are prepared by cost-effective strategy.

The activation energy for Au/STS-1 and Au/HTS-1 catalysts is further compared. The temperature-dependent reaction rate can be used to evaluate the activation energy by Arrhenius equation:

$$\ln(r) = \ln(A) - \frac{E_a}{RT}$$

where r is the reaction rate ($g_{PO}h^{-1}kg_{Cat}^{-1}$), E_a is the activation energy ($kJmol^{-1}$), R is the gas constant (8.3145 $Jmol^{-1}K^{-1}$) and T is the absolute temperature (K). With the increase of reaction temperature from 383 to 473 K, the PO formation rate of Au/STS-1 and Au/HTS-

1 catalysts rise from 21.31 to 140.8 and from 8.64 to 88.2 $g_{PO}h^{-1}kg_{Cat}^{-1}$, respectively. Therefore, the calculated activation energy of Au/STS-1 and Au/HTS-1catalysts are 31.44 and 38.43 kJ/mol, respectively. The lower activation energy of Au/STS-1 confirms that the cost-efficient mesoporous STS-1 supported Au catalyst is more appropriate for gas-phase propene epoxidation with H_2 and O_2.

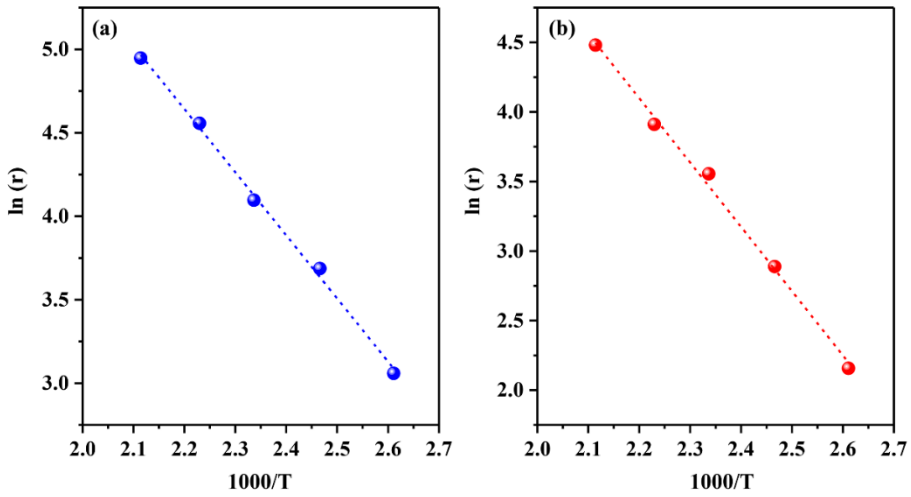

Fig. 8. Different temperature and activation energy on (a) Au/STS-1 and (b) Au/HTS-1 catalysts.

Fig. 9 shows the detailed products selectivities of the Au/STS-1 and Au/HTS-1 catalysts with Au loadings of 0.10 wt% at 473K. The main side products of Au/STS-1 and Au/HTS-1 catalysts are all carbon dioxide and ethanal. Compared with Au/HTS-1 catalyst, the Au/STS-1 catalyst produces higher PO selectivity and fewer side products. This is possibly because during the transmission, the poorer transmission ability of H_2O_2 from Au nanoparticles to the nearby Ti^{4+} centers on larger TS-1 support particles may give rise to the non-selective oxidation of propene to several side products such as CO_2, ethanal and propanal [51,52]. Meanwhile, the better mass transfer ability provided by the smaller particle size and the mesopores can not only promote the transfer of reaction intermediate

between Au nanoparticles and the nearby Ti^{4+} centers, but also facilitates the desorption of PO and inhibits the ring-opening reaction [53,54]. It should be noted that there is no improved stability of our catalyst than the reported conventional Au/TS-1 catalyst. However, methods could be taken to further enhance the stability by reducing the STS-1 size or surface hydrophobicity modification [44].

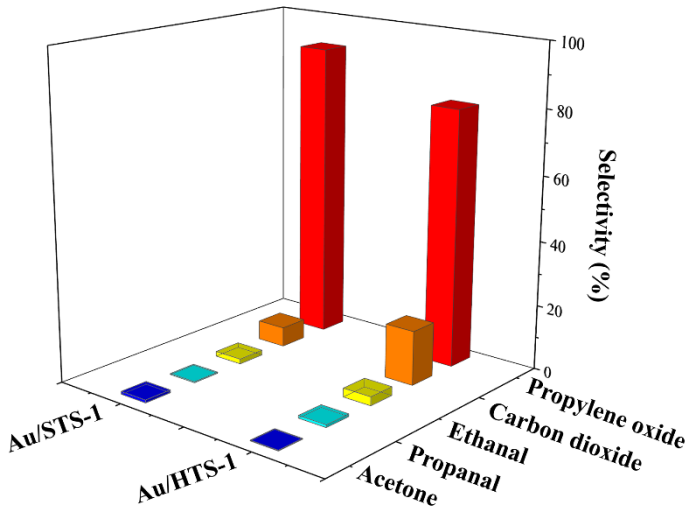

Fig. 9. Detailed products selectivities of Au/STS-1 and Au/HTS-1 catalysts with the same Au loadings of 0.10 wt%

From the above results, it can be seen that the crystal size could be efficiently reduced after the addition of TS-1 seeds. The cost-efficient STS-1 material has small average crystal size of ca. 600 nm on the a-axis. In addition, the SAC method could also create mesopores, which further enhances the effective mass transfer ability. Consequently, the Au/STS-1 catalyst shows good propene epoxidation performance, which is not only much better than Au/HTS-1 catalyst, but also similar to that of conventional Au/TS-1 support at the similar Si/Ti molar ratio. This work is of great essential to the design of highly effective and cost-efficient TS-1 for industrial applications. In recent years, the studies on the design of cost-

effective TS-1 and its catalytic performance have made great progress. However, the catalytic activity, selectivity and stability of the cost-effective TS-1 still need to be further improved. Therefore, the synthesis of cost-effective TS-1 with high catalytic performance still has a long way to go.

4 Conclusions

In summary, small-sized mesoporous TS-1 (STS-1) with pore size of ca. 13 nm and small crystal size (ca. 600 nm on the a-axis) is successfully synthesized using cost-efficient TPABr as template by SAC method with the aid of seeding. Moreover, the TPABr concentration is reduced to an appropriate value to balance the synthetic cost, the physico-chemical properties, morphology and Ti species of STS-1. Notably, it is found that STS-1 supported Au catalyst exhibits good catalytic performance for direct propene epoxidation with H_2 and O_2 with the PO formation rate of 140.8 $g_{PO}h^{-1}kg_{Cat}^{-1}$ and improved PO selectivity of 91.2% which is not only much better than Au/HTS-1 catalyst, but also comparable to the reported conventional expensive Au/TS-1 catalyst with the same Si/Ti molar ratio. The enhanced performance of Au/STS-1 catalyst is also demonstrated by the lower activation energy. This could be due to the Au/STS-1 catalyst has enhanced mass transfer ability by shortened reactant/product diffusion length. The insights reported here may pave the way for the rational design of highly effective and cost-efficient TS-1 for industrial applications.

ACKNOWLEDGMENT

This work is financially supported by the Natural Science Foundation of China (21606254); Natural Science Foundation of Shandong Province (ZR2016BB16); Key research and development plan of Shandong Province (2017GSF17126); Fundamental Research Funds for the Central Universities (18CX02014A); and Independent innovation foundation of Qingdao (17-1-1-18-jch).

REFERENCES

[1] M. Taramasso, G. Perego, B. Notari, Preparation of porous crystalline synthetic material comprised of silicon and titanium oxides, US Patent 4,410,501 (1983).

[2] W. Fan, R. G. Duan, T Yokoi, P. Wu, Y. Kubota, T. Tatsumi, Synthesis, crystallization mechanism, and catalytic properties of titanium-rich TS-1 free of extraframework titanium species. J. Am. Chem. Soc. 130 (2008) 10150-10164.

[3] I. Schmidt, A. Krogh, K. Wienberg, A. Carlsson, M. Brorson, C.J.H. Jacobsen, Catalytic epoxidation of alkenes with hydrogen peroxide over first mesoporous titanium-containing zeolite, Chem. Commun. 21 (2000) 2157-2158.

[4] P. Wu, D. Nuntasri, J. Ruan, Y. Liu, M. He, W. Fan, O. Terasaki, T. Tatsumi, Delamination of Ti-MWW and high efficiency in epoxidation of alkenes with various molecular sizes, J. Phys. Chem. B 108 (2004) 19126-19131.

[5] J.L. Bars, J. Dakka, R.A. Sheldon, Ammoximation of cyclohexanone and hydroxyaromatic ketones over titanium molecular, Appl. Catal. A-Gen. 136 (1996) 69-80.

[6] Y. Zhang, Y. Wang, Y. Bu, L. Wang, Z. Mi, W. Wu, E. Min, S. Fu, Z. Zhu, Reaction mechanism of the ammoximation of ketones catalyzed by TS-1, React. Kinet. Mech. Cat. 87 (2005) 25-32.

[7] R. Kumar, P. Mukherjee, A. Bhaumik, Enhancement in the reaction rates in the hydroxylation of aromatics over TS-1/H_2O_2 under solvent-free triphase conditions, Catal. Today 49 (1999) 185-191.

[8] Kerton, P. Mcmorn, D. Bethell, F. King, F. Hancock, A. Burrows, C.J. Kiely, S. Ellwood, G. Hutchings, Effect of structure of the redox molecular sieve TS-1 on the oxidation of phenol, crotyl alcohol and norbornylene, Phys. Chem. Chem. Phys. 7 (2005) 2671-2678.

[9] S. Heinrich, M. Plettig, E. Klemm, Role of the Ti(IV)-superoxide species in the selective oxidation of alkanes with hydrogen peroxide in the gas phase on titanium silicalite-1: An in situ EPR investigation, Catal. Lett. 141 (2011) 251-258.

[10] X.S. Wang, X.W. Guo, G. Li, Synthesis of titanium silicalite (TS-1) from the TPABr system and its catalytic properties for epoxidation of propylene, Catal. Today 74 (2002) 65-75.

[11] X. Wang, G. Li, W. Wang, C. Jin, Y. Chen, Synthesis, characterization and catalytic performance of hierarchical TS-1 with carbon template from sucrose carbonization, Micropor. Mesopor. Mat. 142 (2011) 494-502.

[12] T. Iwasaki, M. Isaka, H. Nakamura, M. Yasuda, S. Watano, Synthesis of titanosilicate TS-1 crystals via mechanochemical route using low cost materials, Micropor. Mesopor. Mat. 150 (2012) 1-6.

[13] H.S. Yan, J. Liu, X.S. Wang, Study on solvolysis of propylene oxide, Chinese J. Catal. 22 (2001) 250-254.

[14] R. Cai, Y. Liu, S. Gu, Y. Yan, Ambient pressure dry-gel conversion method for zeolite MFI synthesis using ionic liquid and microwave heating, J. Am. Chem. Soc. 132 (2010) 12776-12777.

[15] Sakthivel, A. Iida, K. Komura, Y. Sugi, K.V.R. Chary, Nanosized β-zeolites with tunable particle sizes: Synthesis by the dry gel conversion (DGC) method in the presence of surfactants, characterization and catalytic properties, Micropor. Mesopor. Mat. 119 (2009) 322-330.

[16] S. Shen, F. Chen, P.S. Chow, P. Phanapavudhikul, K. Zhu, R.B.H. Tan, Synthesis of SBA-15 mesoporous silica via dry-gel conversion route, Micropor. Mesopor. Mat. 92 (2006) 300-308.

[17] B.C. And, Y. Huang, Examining the self-assembly of microporous material $AlPO_4$-11 by dry-gel conversion, J. Phys. Chem. C 111 (2007) 15236-15243.

[18] C.M. Song, Y. Feng, L.L. Ma, Characterization and hydroisomerization performance of SAPO-11 molecular sieves synthesized by dry gel conversion, Micropor. Mesopor. Mat. 147 (2012) 205-211.

[19] S.P. Naik, A.S.T. Chiang, R.W. Thompson, Synthesis of zeolitic mesoporous materials by dry gel conversion under controlled humidity, J. Phys. Chem. B 107 (2003) 7006-7014.

[20] Y. Zuo, X. Wang, X. Guo, Synthesis of titanium silicalite-1 with small crystal size by using mother liquid of titanium silicalite-1 as seed, Ind. Eng. Chem. Res. 50 (2011) 8485–8491.

[21] X. Feng, X. Duan, Q. Gang, X. Zhou, D. Chen, W. Yuan, Au nanoparticles deposited on the external surfaces of TS-1: Enhanced stability and activity for direct propylene epoxidation with H_2 and O_2, Appl. Catal. B-Environ. 150-151 (2014) 396-401.

[22] K. Takemura, Evaluation of the hydrostaticity of a helium-pressure medium with powder X-ray diffraction techniques, J. Appl. Phys. 89 (2001) 662-668.

[23] S. Bordiga, F. Bonino, A. Damin, C. Lamberti, Reactivity of Ti(IV) species hosted in TS-1 towards H_2O_2-H_2O solutions investigated by ab initio cluster and periodic approaches combined with experimental XANES and EXAFS data: A review and new highlights, Phys. Chem. Chem. Phys. 9 (2007) 4854-4878.

[24] J. Su, G. Xiong, J. Zhou, W. Liu, D. Zhou, G. Wang, X. Wang, H. Guo, Amorphous Ti species in titanium silicalite-1: Structural features, chemical properties, and inactivation with sulfosalt, J. Catal. 288 (2012) 1-7.

[25] T. Zhang, Y. Zuo, M. Liu, C. Song, X. Guo, Synthesis of titanium silicalite-1 with high catalytic performance for 1-butene epoxidation by eliminating the extraframework Ti, ACS Omega 1 (2016) 1034-1040.

[26] T. Armaroli, F. Milella, B. Notari, R.J. Willey, G. Busca, A spectroscopic study of amorphous and crystalline Ti-containing silicas and their surface acidity, Top. Catal. 15 (2001) 63-71.

[27] G.N. Vayssilov, Structural and physicochemical features of titanium silicalites, Catal. Rev. 39 (1997) 209-251.

[28] L. Xu, Y. Ren, H. Wu, Y. Liu, Z. Wang, Y. Zhang, J. Xu, H. Peng, P. Wu, Core/shell-structured TS-1@mesoporous silica-supported Au nanoparticles for selective epoxidation of propylene with H_2 and O_2, J. Mater. Chem. 21 (2011) 10852-10858.

[29] Z. Wang, L. Xu, J.G. Jiang, Y. Liu, M. He, P. Wu, One-pot synthesis of catalytically active and mechanically robust mesoporous TS-1 microspheres with the aid of triblock copolymer, Micropor. Mesopor. Mat. 156 (2012) 106-114.

[30] D.P. Serrano, R. Sanz, P. Pizarro, I. Moreno, S. Medina, Hierarchical TS-1 zeolite as an efficient catalyst for oxidative desulphurization of hydrocarbon fractions, Appl. Catal. B-Environ. 146 (2014) 35-42.

[31] E. Jorda, A. Tuel, R. Teissier, J. Kervennal, TiF4: An original and very interesting precursor to the synthesis of titanium containing silicalite-1, Micropor. Mesopor. Mat. 19 (1997) 238-245.

[32] C. Perego, A. Carati, P. Ingallina, M.A. Mantegazza, G. Bellussi, Production of titanium containing molecular sieves and their application in catalysis, Appl. Catal. A-Gen. 221 (2001) 63-72.

[33] C. Shen, Y. Wang, J. Xu, G. Luo, Synthesis of TS-1 on porous glass beads for catalytic oxidative desulfurization, Chem. Eng. J. 259 (2015) 552-561.

[34] X. Li, Y. Peng, Z. Wang, Y. Yan, Synthesis of highly b-oriented zeolite MFI films by suppressing twin crystal growth during the secondary growth, CrystEngComm 13 (2011) 3657-3660.

[35] Y. Hirota, K. Murata, S. Tanaka, N. Nishiyama, Y. Egashira, K. Ueyama, Dry gel conversion synthesis of SAPO-34 nanocrystals, Mater. Chem. Phys. 123 (2010) 507-509.

[36] S. Alfaro, M.A. Valenzuela, P. Bosch, Synthesis of silicalite-1 by dry-gel conversion method: Factors affecting its crystal size and morphology, J. Porous Mater. 16 (2009) 337-342.

[37] Q. Du, Y. Guo, P. Wu, H. Liu, Synthesis of hierarchically porous TS-1 zeolite with excellent deep desulfurization performance under mild conditions, Micropor. Mesopor. Mat. (2018).

[38] L. Ding, Y. Zheng, Effect of template concentration and gel dilution on crystallization and particle size of zeolite beta in the absence of alkali cations, Micropor. Mesopor. Mat. 103 (2007) 94-101.

[39] Z.A.D. Lethbridge, J.J. Williams, R.I. Walton, K.E. Evans, C.W. Smith, Methods for the synthesis of large crystals of silicate zeolites, Micropor. Mesopor. Mat. 79 (2005) 339-352.

[40] S. Mintova, J.P. Gilson, V. Valtchev, Advances in nanosized zeolites, Nanoscale 5 (2013) 6693-6703.

[41] T.A. Nijhuis, M. Makkee, J.A. Moulijn, B.M. Weckhuysen, The production of propene oxide: Catalytic processes and recent developments, Ind. Eng. Chem. Res. 45 (2006) 3447-3459.

[42] J. Huang, E. Lima, T. Akita, A. Guzmán, C. Qi, T. Takei, M. Haruta, Propene epoxidation with O_2 and H_2: Identification of the most active gold clusters, J. Catal. 278 (2011) 8-15.

[43] W.S. Lee, M.C. Akatay, E.A. Stach, F.H. Ribeiro, W.N. Delgass, Enhanced reaction rate for gas-phase epoxidation of propylene using H_2 and O_2 by Cs promotion of Au/TS-1, J. Catal. 308 (2013) 98-113.

[44] X. Feng, N. Sheng, Y. Liu, X. Chen, D. Chen, C. Yang, X. Zhou, Simultaneously enhanced stability and selectivity for propene epoxidation with H_2 and O_2 on Au catalysts supported on nano-crystalline mesoporous TS-1, ACS Catal. 7 (2017) 2668-2675.

[45] Z. Song, X. Feng, Y. Liu, C. Yang, X. Zhou, Advances in Manipulation of catalyst structure and relationship of structure-performance for direct propene epoxidation with H_2 and O_2, Prog. Chem. 28 (2016) 1762-1773.

[46] X. Feng, X. Duan, G. Qian, X. Zhou, D. Chen, W. Yuan, Insights into size-dependent activity and active sites of Au nanoparticles supported on TS-1 for propene epoxidation with H_2 and O_2, J. Catal. 317 (2014) 99-104.

[47] X. Feng, X. Duan, H Cheng, G. Qian, D. Chen, W. Yuan, X. Zhou, Au/TS-1 catalyst prepared by deposition–precipitation method for propene epoxidation with H_2/O_2: Insights into the effects of slurry aging time and Si/Ti molar ratio, J. Catal. 325 (2015) 128-135.

[48] W.S. Lee, M.C. Akatay, E.A. Stach, F.H. Ribeiro, W.N. Delgass, Reproducible preparation of Au/TS-1 with high reaction rate for gas phase epoxidation of propylene, J. Catal. 287 (2012) 178-189.

[49] J. Huang, T. Takei, T. Akita, Gold clusters supported on alkaline treated TS-1 for highly efficient propene epoxidation with O_2 and H_2, Appl. Catal. B-Environ. 95 (2010) 430-438.

[50] Y. Liu, X. Zhang, J. Suo, Gold supported on nitrogen-incorporated TS-1 for gas-phase epoxidation of propylene, Chinese J. Catal. 34 (2013) 336-340.

[51] X. Feng, Y. B. Liu, Y. C. Li, C.H. Yang, Z.H Zhang, X.Z. Duan, X.G Zhou, Au/TS‐1 catalyst for propene epoxidation with H_2/O_2: A novel strategy to enhance stability by tuning charging sequence, AIChE J. 62 (2016) 3963-3972.

[52] X. Feng, X. Duan, J. Yang, G. Qian, X. Zhou, D. Chen, W. Yuan, Au/uncalcined TS-1 catalysts for direct propene epoxidation with H_2 and O_2: effects of Si/Ti molar ratio and Au loading, Chem. Eng. J. 278 (2015) 234-239.

[53] A. Ruiz, B.V.D. Linden, M. Makkee, G. Mul, Acrylate and propoxy-groups: Contributors to deactivation of Au/TiO_2 in the epoxidation of propene, J. Catal. 266 (2009) 286-290.

[54] X. Feng, D. Chen, X. Zhou, Thermal stability of TPA template and size-dependent selectivity of uncalcined TS-1 supported Au catalyst for propene epoxidation with H_2 and O_2, Rsc Adv. 50 (2016) 44050-44056.